Enhancing calstabin binding to ryanodine receptors improves cardiac and skeletal muscle function in heart failure

Xander H. T. Wehrens*, Stephan E. Lehnart*, Steven Reiken*, Roel van der Nagel†, Raymond Morales*, Jie Sun‡, Zhenzhuang Cheng‡, Shi-Xiang Deng‡, Leon J. de Windt†, Donald W. Landry‡, and Andrew R. Marks*‡§

Departments of *Physiology and Cellular Biophysics and ‡Medicine, College of Physicians and Surgeons, Columbia University, New York, NY 10032; and †Hubrecht Laboratory, Royal Netherlands Academy of Arts and Sciences, 3584CT, Utrecht, The Netherlands

Abnormalities in intracellular calcium release and reuptake are responsible for decreased contractility in heart failure (HF). We have previously shown that cardiac ryanodine receptors (RyRs) are protein kinase A-hyperphosphorylated and depleted of the regulatory subunit calstabin-2 in HF. Moreover, similar alterations in skeletal muscle RyR have been linked to increased fatigability in HF. To determine whether restoration of calstabin binding to RyR may ameliorate cardiac and skeletal muscle dysfunction in HF, we treated WT and calstabin-2$^{-/-}$ mice subjected to myocardial infarction (MI) with JTV519. JTV519, a 1,4-benzothiazepine, is a member of a class of drugs known as calcium channel stabilizers, previously shown to increase calstabin binding to RyR. Echocardiography at 21 days after MI demonstrated a significant increase in ejection fraction in WT mice treated with JTV519 (45.8 ± 5.1%) compared with placebo (31.1 ± 3.1%; $P < 0.05$). Coimmunoprecipitation experiments revealed increased amounts of calstabin-2 bound to the RyR2 channel in JTV519-treated WT mice. However, JTV519 did not show any of these beneficial effects in calstabin-2$^{-/-}$ mice with MI. Additionally, JTV519 improved skeletal muscle fatigue in WT and calstabin-2$^{-/-}$ mice with HF by increasing the binding of calstabin-1 to RyR1. The observation that treatment with JTV519 improved cardiac function in WT but not calstabin-2$^{-/-}$ mice indicates that calstabin-2 binding to RyR2 is required for the beneficial effects in failing hearts. We conclude that JTV519 may provide a specific way to treat the cardiac and skeletal muscle myopathy in HF by increasing calstabin binding to RyR.

calcium | FKBP12.6 | myocardial infarction | contractility

Heart failure (HF) is the leading cause of death in the Western world (1), and there is a lack of therapeutic agents that specifically target the underlying cellular defects (2). The primary abnormality is impaired contractile function of the heart, which leads to the activation of compensatory mechanisms, such as increased sympathetic nervous system activity (3). In addition, some of the major symptoms in HF are caused by skeletal muscle dysfunction (e.g., shortness of breath due to diaphragmatic weakness and exercise intolerance due to limb skeletal muscle fatigue) (4).

It is generally agreed that much of the contractile dysfunction is caused by reduced myocyte calcium (Ca^{2+}) transients (5). The sarcoplasmic reticulum (SR) Ca^{2+} content reflects the balance between Ca^{2+} uptake [by means of SR calcium ATPase (SERCA)] and Ca^{2+} efflux [by means of ryanodine receptors (RyRs)]. Therefore, a reduced SR content in HF may be due to reduced Ca^{2+} pumping by SERCA2a or increased SR Ca^{2+} leak by RyRs. Experimental evidence for both mechanisms has been reported in humans with HF and relevant animal models (6, 7). In addition, reduced sarcolemmal Ca^{2+} influx (through L-type Ca^{2+} channels) (5) or enhanced cytoplasmic Ca^{2+} extrusion (by Na^+/Ca^{2+} exchange) may unload the SR (8). Although recent studies have identified abnormal regulation of intracellular Ca^{2+} release from the SR as a pathogenic mechanism underlying both cardiac and

skeletal muscle dysfunction in patients with HF (7, 9–11), other studies have raised controversy as to the importance of SR Ca^{2+} leak in HF (12–14).

Calcium release channels (RyR) on the SR of striated muscles are required for excitation–contraction coupling and play an important role in regulating striated muscle contraction (15). In cardiac muscle, RyR2 constitutes a homotetrameric channel comprised of four RyR2 monomers, each binding a Ca^{2+} channel-stabilizing subunit, calstabin-2 (also known as FKBP12.6) (16). Accordingly, skeletal muscle RyR1 comprises a homotetrameric channel binding four calstabin-1 (FKBP12) subunits (17). Although the FK506-binding proteins FKBP12 and FKBP12.6 are members of the immunophilin protein family and serve as cytosolic receptors for immunosuppressant drugs, we recently proposed the name calstabin for its physiological cellular function in the RyR channel complex (18, 19). During the resting phase after each muscle contraction, binding of calstabin to RyR helps maintain the channel in a closed state to prevent leakage of SR Ca^{2+} into the cytoplasm (20).

In previous studies, we have shown that chronic hyperactivity of the sympathetic nervous system in HF induces structural changes in cardiac and skeletal muscle RyR channel complexes, which include hyperphosphorylation by protein kinase A (PKA) and dissociation of the channel-stabilizing subunit calstabin (7, 10). These HF-induced modifications result in RyR/Ca^{2+} release channels that may become "leaky" during diastole, because binding of calstabin to RyR is required to stabilize the closed state of the channel, which occurs during diastole in the heart (7, 9, 21). According to the diastolic SR Ca^{2+} leak theory, chronic diastolic SR Ca^{2+} leak in HF is believed to reduce the SR Ca^{2+} content, which contributes to reduced Ca^{2+} transients and weaker muscle contraction in cardiac and skeletal muscle (7, 9–11). Indeed, recent studies have confirmed major aspects of this model by showing that there is a SR Ca^{2+} leak and depleted SR Ca^{2+} content in failing hearts (11). Moreover, in the heart, aberrant diastolic Ca^{2+} release through leaky RyR2 can trigger fatal cardiac arrhythmias, (19, 22) which are known to cause up to 50% of all sudden deaths in patients with HF (23).

We recently demonstrated that the 1,4-benzothiazepine JTV519, a member of a class of drugs known as calcium channel stabilizers, prevents catecholamine-induced ventricular arrhythmias in calstabin-2 haploinsufficient mice (19). JTV519 prevented diastolic Ca^{2+} leak and arrhythmias by increasing the binding affinity of calstabin-2 for PKA-phosphorylated RyR2. JTV519 has also been shown

MEDICAL SCIENCES

to inhibit the progression of pacing-induced HF in dogs by reducing SR Ca^{2+} leak, presumably by enhancing calstabin-2 binding to RyR2 (24). However, it is unclear at present whether the effect of JTV519 in HF depends on rebinding of calstabin-2 to PKA-hyperphosphorylated RyR2. Also, because of the controversy over the potential role of PKA hyperphosphorylation-mediated dissociation of calstabin-2 from RyR2 in HF (5, 12, 14), it is important to ask whether a treatment that may restore binding of calstabin to RyR can improve striated muscle function in HF. Additionally, it is unknown whether JTV519 may enhance binding of calstabin-1 to RyR1, which could potentially improve skeletal muscle function in HF. Therefore, we examined the efficacy of JTV519 in a mouse model of ischemia-induced HF. Calstabin-2$^{-/-}$ mice were used to investigate whether the action of JTV519 depends on enhanced calstabin binding to RyR in cardiac and skeletal muscle.

Materials and Methods

Surgical Procedure and Animal Models. Calstabin-2$^{-/-}$ mice (22) and WT littermates were maintained and studied according to protocols approved by the Institutional Animal Care and Use Committee of Columbia University. Mice were randomized to receive either myocardial infarction (MI) or a sham procedure. Mice were anesthetized by using 1.5% isoflurane in O_2, cannulated, and ventilated with a tidal volume of 0.3 ml (180 strokes per min). A left lateral thoracotomy was performed between the fourth and fifth ribs, and the left anterior descending artery was visualized and permanently ligated proximally with a 8-0 silk suture. Sham-operated animals underwent the same procedure without occlusion of the left anterior descending artery. The chest was closed, the lung was reinflated, and the animal was moved to a prone position until spontaneous breathing occurred.

Drugs. The 1,4-benzothiazepine JTV519 was synthesized as described in ref. 19. JTV519 was continuously infused for 4 weeks (0.5 mg·kg^{-1}·h^{-1}) in mice by means of an implantable osmotic infusion pump (Alzet MiniOsmotic pump, Durect, Cupertino, CA). The solvent for JTV519 used in these experiments (DMSO) served as placebo.

Transthoracic Echocardiography. Twenty-one days after MI, mice were anesthetized with 1.5% isoflurane in O_2 and placed on a heating pad (37°C). Hearts were visualized with a Hewlett–Packard Sonos 5500 ultrasound machine with a 12-MHz transducer applied parasternally to the chest wall. Cardiac ventricular dimensions were measured on M-mode three times for the number of animals indicated.

Hemodynamic Analysis. Twenty-eight days after MI, the mice were anesthetized with 1.5% isoflurane and placed on a heating pad (37°C). A 1.4-F high-fidelity micromanometer catheter (Millar Instruments, Houston, TX) was introduced into the right carotid artery and advanced across the aortic valve into the left ventricular cavity (25).

Skeletal Muscle Function. Soleus muscles were attached to a force transducer in a muscle bath (Harvard Apparatus) and perfused with Tyrode solution containing 2 mM Ca^{2+} gassed with 100% O_2 (10). After equilibration for 30 min, the muscle was stimulated with single pulses at 10-s intervals to determine stimulation threshold. Fatigue was produced by a tetanus protocol (50 Hz, 600 ms) every 2 s under isometric conditions, and fatigue time was determined at 50% reduction of the maximal tetanic force.

Histological Analysis. After invasive hemodynamic analysis, the hearts were arrested in diastole and perfused antegradely at physiological pressures with PBS containing 0.5 mM KCl. Heart tissue was fixed in 3.7% buffered formalin, cut transversely through the maximal diameter of the infarcted area, and embedded in paraffin. Sections (4 μm) were stained with hematoxylin and eosin, and infarct size was calculated as a total infarct circumference divided by total left ventricular circumference.

Immunoprecipitation and Western Blot Analysis. RyR channels were immunoprecipitated from 100 μg of cardiac or skeletal muscle homogenates with anti-RyR antibody (17) in 0.5 ml of buffer (50 mM Tris·HCl buffer, pH 7.4/0.9% NaCl/5.0 mM NaF/1.0 mM Na_3VO_4/0.25% Triton X-100/protease inhibitors) overnight at 4°C. The samples were incubated with protein A Sepharose beads (Amersham Pharmacia) at 4°C for 1 h, after which the beads were washed three times with buffer. Proteins were separated on SDS/PAGE gels (6% for RyR2 and 15% for calstabin-2/calstabin-1) and transferred onto nitrocellulose membranes overnight (SemiDry transfer blot, Bio-Rad). After incubation with 5% nonfat milk to prevent aspecific antibody binding and a wash in Tris-buffered saline with 0.1% Tween 20, membranes were incubated for 1–2 h at room temperature with primary antibodies anti-calstabin (1:1,000) (22), anti-RyR (5029; 1:3,000) (17), or anti-phospho-RyR2-pSer^{2809} (1:5,000), which detects PKA-phosphorylated mouse RyR1-pSer^{2844} and RyR2-pSer^{2808} (21). After three washes, membranes were incubated with horseradish peroxidase-labeled anti-rabbit IgG (1:5,000, Transduction Laboratories, Lexington, KY), and developed with an enhanced chemiluminescent detection system (Amersham Pharmacia). Band densities were quantified by using QUANTITY ONE software (Bio-Rad) (26).

Calstabin Affinity Assay. RyR1 or RyR2 was phosphorylated with PKA catalytic subunit (40 units; Sigma) in the presence or absence of the PKA inhibitor PKI$_{5-24}$ in phosphorylation buffer (8 mM $MgCl_2$/10 mM EGTA/50 mM Tris/Pipes, pH 6.8). ^{35}S-labeled calstabin-1 or calstabin-2 were generated by using the TNT Quick Coupled Transcription/Translation system from Promega (19). [^{3}H]ryanodine binding was used to quantify RyR levels. Microsomes (100 μg) were diluted in 100 μl of 10 mM imidazole buffer, pH 6.8, and incubated with 250 nM (final concentration) [^{35}S]calstabin at 37°C for 60 min, then quenched with 500 μl ice-cold imidazole buffer. Samples were centrifuged at 100,000 × g for 10 min and washed three times in imidazole buffer, and the amount of bound [^{35}S]calstabin was determined by liquid scintillation counting of the pellet.

Single-Channel Recordings. Vesicles containing RyR2 or RyR1, respectively, were incorporated into planar lipid bilayers in 100-μm holes in polystyrene cups separating two chambers. The trans chamber (1.0 ml), representing the intra-SR compartment, was connected to the head stage input of a bilayer voltage-clamp amplifier (Warner Instruments, Hamden, CT). The cis chamber (1.0 ml), representing the cytoplasmic compartment, was held at virtual ground. Symmetrical solutions used are as follows: trans, 250 mM Hepes/53 mM Ca(OH)$_2$, pH 7.35; cis, 250 mM Hepes/125 mM Tris/1.0 mM EGTA/0.5 mM $CaCl_2$, pH 7.35. At the conclusion of each experiment, 5 μM ryanodine or 20 μM ruthenium red was applied to confirm RyR2 channel identity.

Statistical Analysis. Statistical analyses between the experimental groups were performed by using a Student's t test or one-way ANOVA when comparing multiple groups. Data are reported as mean ± SEM. Values of P at ≤0.05 were considered significant.

Results

Characterization of Cardiac Function in WT and Calstabin2$^{-/-}$ Mice with MI. There was a trend toward decreased survival in calstabin-2$^{-/-}$ compared with WT mice at 28 days after MI (Fig. 1A), although this study did not have enough power to uncover statistically significant differences. Nevertheless, this finding suggests that the loss of calstabin-2 binding to RyR2 may worsen the development of HF in mice subjected to MI and that enhancing the
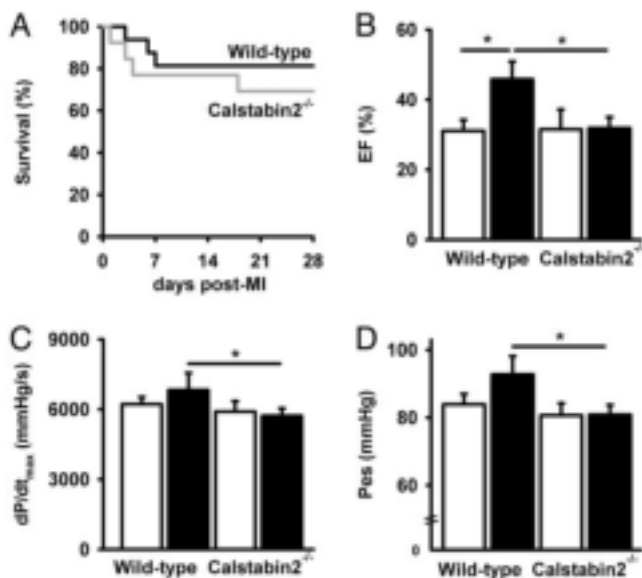
Fig. 1. Increased cardiac function and reverse remodeling in mice treated with JTV519 3 weeks after MI. (A) Kaplan–Meier survival curve for WT and calstabin-2$^{-/-}$ mice after permanent coronary artery ligation resulting in MI. (B) Quantification of M-mode echocardiograms showing improved ejection fraction (EF) in JTV519-treated WT mice compared with placebo. *, $P < 0.05$. (C and D) Pressure–volume loop quantifications showing improved cardiac function in JTV519-treated WT compared with calstabin-2$^{-/-}$ mice. dP/dt$_{max}$, slope of the maximum derivative of change in systolic pressure over time; Ped, end-systolic pressure; *, $P < 0.05$.

binding of calstabin-2 to RyR2 may be therapeutic in HF. Indeed, cardiac function 21 days after MI was improved as evidenced by increased fractional shortening (+62%) and ejection fraction (+47%) in JTV519-treated WT mice compared with placebo (Fig. 1 A and B and Table 1, which is published as supporting information on the PNAS web site). In contrast, JTV519 did not enhance cardiac function in calstabin-2$^{-/-}$ mice. Hemodynamic responses were assessed in WT and calstabin-2$^{-/-}$ mice 28 days after MI (Fig. 1 C and D). Treatment with JTV519 significantly ameliorated the maximal change in systolic pressure over time (dP/dt$_{max}$) in JTV519-treated WT mice [6,826 ± 735 mmHg/s (1 mmHg = 133 Pa)] compared with calstabin-2$^{-/-}$ mice (5,726 ± 314 mmHg/s; $P < 0.05$). Moreover, there was a significant decrease in heart weight (HW), HW divided by body weight, and HW divided by tibia length in JTV519-treated WT mice with MI compared with placebo (Table 1). However, JTV519 did not prevent cardiac hypertrophy and failure in calstabin-2$^{-/-}$ mice. Taken together, these data suggest that calstabin-2 may be required for the beneficial effects of JTV519 after MI.

Increased Calstabin-2 Binding to RyR2 in Hearts of JTV519-Treated Mice with MI Normalizes RyR2 Channel Function. We have previously shown that calstabin-2 stabilizes the RyR2 channel in the closed state (16, 22) and that PKA phosphorylation of RyR2 at Ser-2808 (Ser-2809 in humans) causes dissociation of calstabin-2 from the channel complex (7, 22). Compared with RyR2 channels from sham-operated mice, RyR2 were significantly PKA-hyperphosphorylated in mice with MI (Fig. 2 A and B). Treatment with JTV519 decreased the level of PKA phosphorylation in WT mice with MI (Fig. 2B), which is believed to be an indirect effect of improved cardiac function resulting in reduced sympathetic stimulation in this group of mice. Compared with channel complexes from sham-operated WT mice, RyR2 complexes from WT mice with MI were significantly more depleted of calstabin-2 (Fig. 2 A and C). Treatment with JTV519, however, increased the amount of calstabin-2 in
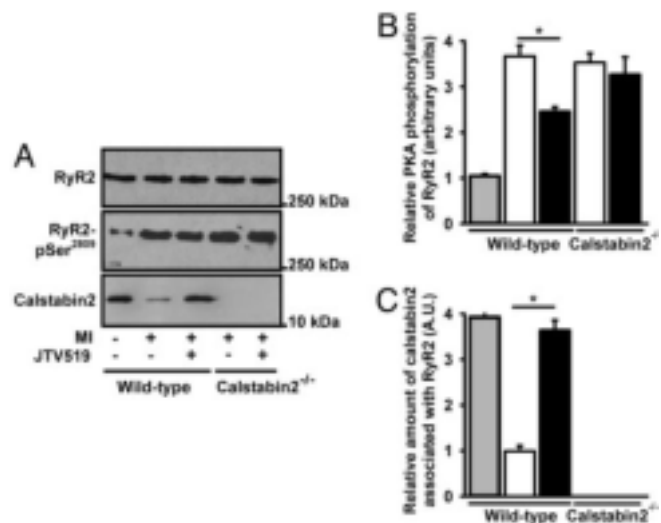

Fig. 2. Effect of JTV519 on calstabin-2 affinity to RyR2 in mice with HF. (A) Equivalent amounts of RyR2 were immunoprecipitated with an antibody against RyR2 (top blot). Representative immunoblots (A) and bar graphs (B and C) show the amount of PKA phosphorylation of RyR2 at Ser-2808 (B) and the amount of calstabin-2 (C) bound to RyR2 from WT or calstabin-2$^{-/-}$ mice treated with JTV519 or placebo. Animals were treated with JTV519 by implantable osmotic pumps (0.5 mg·kg^{-1}·h^{-1} for 28 days after MI).

the RyR2 macromolecular complex 28 days after MI in WT mice (Fig. 2 A and C).

We examined RyR2 single channels in the presence of low cytosolic Ca^{2+} (150 nM) by using Ca^{2+} as the charge carrier. These Ca^{2+} concentrations mimic those in the heart during diastole, when the RyR2 channels should have a low open probability, P_o to prevent diastolic Ca^{2+} leak from the SR (19). The P_o for RyR2 channels from WT mice subjected to MI treated with JTV519 were significantly reduced compared with those of channels from placebo-treated WT mice, consistent with increased amounts of calstabin-2 in the RyR2 channel complex (Fig. 3). In contrast, JTV519 treatment of calstabin-2$^{-/-}$ mice subjected to MI did not result in channels with a low P_o during diastole (Fig. 3). The average P_o values were 0.48 ± 0.08 for placebo-treated WT ($n = 10$), 0.03 ± 0.02 for JTV519-treated WT ($n = 8$; $P < 0.001$ placebo versus JTV519), and 0.45 ± 0.10 for JTV519-treated calstabin-2$^{-/-}$ mice ($n = 7$). Consistent with previous studies showing subconductance states in RyR2 channels depleted from calstabin-2, we observed subconductance states in placebo-treated WT mice with HF (Fig. 3 Top). Because treatment with JTV519 resulted in calstabin-2 binding to RyR2, subconductance states were not observed in JTV519-treated WT mice (Fig. 3 Middle). The significant reduction in the RyR2 P_o observed in JTV519-treated WT mice suggests that channel leak will not occur during diastole, consistent with the finding that cardiac contractility was improved.

Increased Calstabin-1 Binding to RyR1 in Skeletal Muscle of JTV519-Treated Mice with HF Is Associated with Improved Skeletal Muscle Function. We sought to determine whether RyR1 channels from skeletal muscle from mice with HF were PKA-hyperphosphorylated and depleted of calstabin-1, as we previously described for a pacing-induced canine model of HF and a rat model of HF (10). PKA phosphorylation of RyR1 from hind-limb skeletal muscle from mice 28 days after MI was assessed by using immunoprecipitation of RyR1 followed by Western blotting using a phospho-epitope-specific antibody that recognizes the PKA-phosphorylated Ser-2844 on mouse RyR1 (21). RyR1 from mice with HF after MI was PKA-hyperphosphorylated compared with RyR1 from sham-operated normal mice (Fig. 4 A and B): sham, 1.0 ± 0.1; placebo-
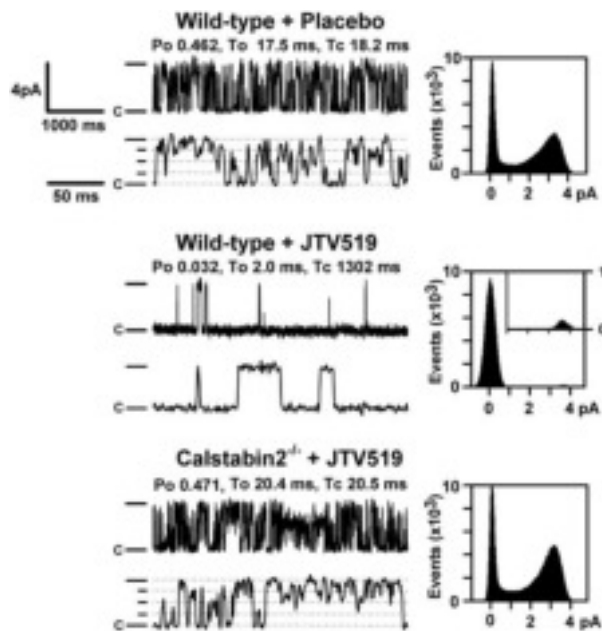
Fig. 3. Normalized RyR2 channel gating in JTV519-treated WT mice with HF. RyR2 channels isolated from hearts 28 days after MI showing normal (low) P_o in WT mice treated with JTV519. Representative single-channel tracings are shown at 150 nM Ca^{2+}. (*Left*) Channel openings are upward, the dash indicates the full level of channel opening (4 pA), the dotted lines indicate subconductance levels, and ''c'' indicates the closed state of the channels. (*Right*) For the amplitude histograms, amplitude is represented on the x axis and ''events'' indicates the number of channel openings. P_o, T_o, and T_c values correspond to the representative tracings shown; average data for all channels were measured as indicated in the text.

treated WT mice with HF, 2.5 ± 0.1 mol of phosphate transferred per mole of RyR1 channel (sham, $n = 7$; HF, $n = 7$; $P < 0.05$). Thus, MI-induced cardiac dysfunction caused PKA hyperphosphorylation of RyR1 in skeletal muscle, in agreement with previous observations in dogs and rats (10).
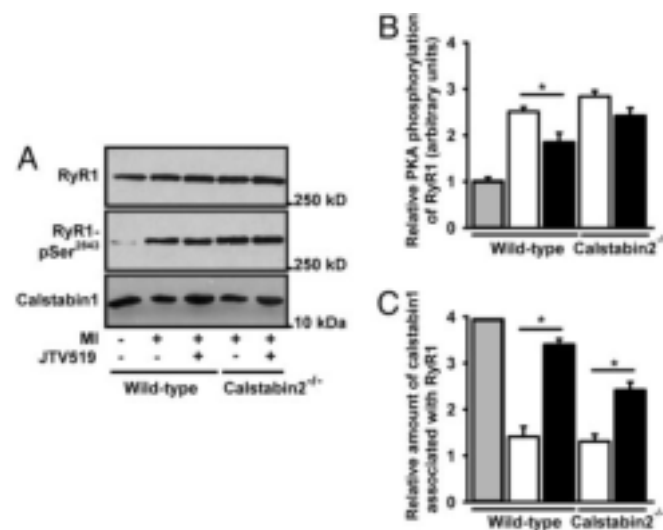

Fig. 4. Increased calstabin-1 binding to RyR1 in soleus muscle after treatment with JTV519. (*A*) Equivalent amounts of RyR2 were immunoprecipitated with an antibody against RyR1 (top blot). Representative immunoblots (*A*) and bar graphs (*B* and *C*) show the amount of PKA phosphorylation of RyR1 at Ser-2844 (*B*) and the amount of calstabin-1 bound to RyR1 (*C*) from WT or calstabin-$2^{-/-}$ mice treated with JTV519 or placebo. Mice were treated with JTV519 by implantable osmotic pumps (0.5 mg·kg^{-1}·h^{-1} for 28 days after MI).
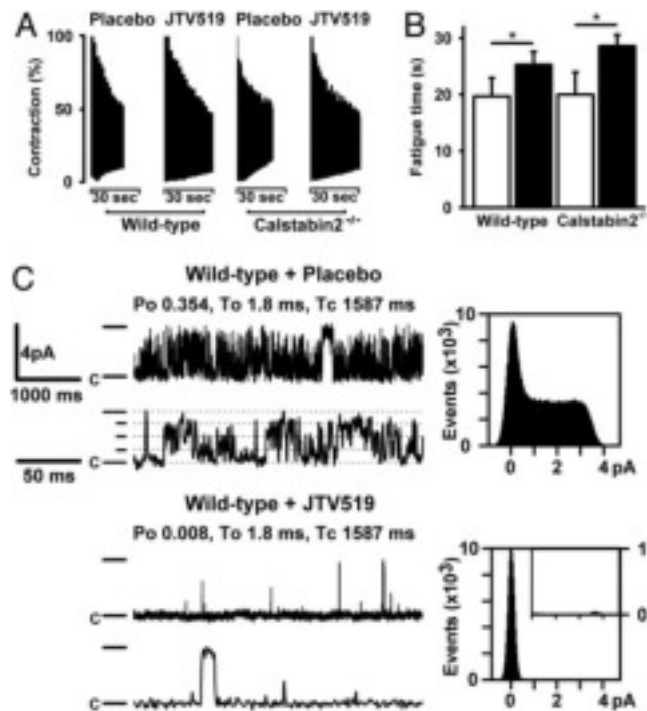

Fig. 5. Reduced fatigability and normalized RyR1 single-channel gating in HF mice treated with JTV519. (*A*) Soleus muscles from JTV519-treated WT mice with HF are more resistant to fatigue compared with placebo. Representative fatigue time tracing is shown for WT and calstabin-$2^{-/-}$ mice treated with JTV519 or placebo. (*B*) Bar graph shows mean ($\pm$SEM) time to fatigue. *, $P < 0.05$. (*C*) Representative RyR1 single-channel tracings are shown at 150 nM Ca^{2+}. Treatment with JTV519 of mice with HF normalized RyR1 channel gating in skeletal muscle. (*Left*) Channel openings are upward, the dash indicates the full level of channel opening (4 pA), the dotted lines indicate subconductance levels, and ''c'' indicates the closed state of the channels. (*Right*) For the amplitude histograms, amplitude is represented on the x axis, and ''events'' indicates the number of channel openings. P_o, T_o, and T_c values correspond to the representative tracings shown; average data for all channels were measured as indicated in the text.

By using coimmunoprecipitations (7), we found that there was a significant reduction ($\approx$4-fold) in the amount of calstabin-1 in the RyR1 macromolecular complex from HF skeletal muscle compared with sham-operated control mice (sham, $n = 7$; HF, $n = 7$; $P < 0.05$) (Fig. 4 *A* and *C*). The total amount of cellular calstabin-1 was not changed (data not shown). Thus, PKA hyperphosphorylation of RyR1 is associated with depletion of calstabin-1 from the RyR1 channel complex in HF skeletal muscle, analogous to the PKA hyperphosphorylation-induced depletion of calstabin-2 from RyR2 in failing hearts (7, 10).

We next sought to determine whether increased binding of calstabin-1 to RyR1 in JTV519-treated HF mice is associated with improved skeletal muscle function. In WT mice, the 50% fatigue time of soleus muscle was 19.7 ± 3.3 s for placebo-treated mice compared with 25.3 ± 2.3 s for JTV519-treated mice ($P < 0.05$) (Fig. 5 *A* and *B*). Interestingly, in calstabin-$2^{-/-}$ mice, the fatigue time also significantly improved in JTV519-treated mice (28.6 ± 2.0 s) compared with placebo (20.0 ± 4.0 s) (Fig. 5 *A* and *B*). JTV519 did not improve cardiac function in calstabin-$2^{-/-}$ mice with HF, which suggests that JTV519 has a beneficial effect on skeletal muscle function in HF, independent from potential beneficial effects on the heart itself.

The P_o values for single RyR1 channels isolated from soleus muscle from WT mice subjected to MI treated with JTV519 were significantly reduced (0.008 ± 0.003) compared with those of channels from placebo-treated WT mice (0.35 ± 0.05; $P < 0.05$)

(Fig. 5C). These observations are consistent with increased amounts of calstabin-1 in the RyR1 channel complex in JTV519-treated HF mice (Fig. 4). Moreover, JTV519 treatment of calstabin-$2^{-/-}$ mice subjected to MI also resulted in channels with a low P_o during diastole (data not shown).

JTV519 Increases the Calstabin-1 Binding Affinity to RyR1. To further examine the mechanisms by which JTV519 improves skeletal muscle function in HF (10, 27), we simulated the HF conditions by using PKA phosphorylation of membrane preparations of mouse skeletal muscle containing RyR1 channels. PKA-phosphorylated RyR1 channels were incubated with 250 nM calstabin-1 in the presence of various concentrations of JTV519. Incubation of PKA-phosphorylated RyR1 channels and calstabin-1 with ≥50 nM of JTV519 induced binding of calstabin-1 to RyR1 (Fig. 6, which is published as supporting information on the PNAS web site). Identical experiments were performed by using membrane preparations of mouse myocardium containing RyR2 channels. Similar to the effects of JTV519 on calstabin-1-RyR1 binding, incubation of PKA-phosphorylated RyR2 channels and calstabin-2 with ≥50 nM of JTV519 induced binding of calstabin-2 to RyR2.

We have previously shown that the affinity of calstabin-2 for PKA-phosphorylated RyR2 channels is significantly increased by the addition of JTV519 (19). The dissociation constants (K_d values) for calstabin-1 binding to nonphosphorylated or PKA-phosphorylated mouse skeletal muscle RyR1 channels were as follows: 93.8 ± 4.0 nM for RyR1 plus PKA and PKI$_{5-24}$ (PKA inhibitor); 1,068.5 ± 77.5 nM for RyR1 plus PKA; and 110.3 ± 1.8 nM for RyR1 plus PKA and JTV519 (each n = 3; P < 0.05) (Fig. 6B, which is published as supporting information on the PNAS web site). These results are similar for mouse cardiac RyR2 channels; K_d values for calstabin-2 binding were 116.6 ± 5.4 nM for RyR2 plus PKA and PKI$_{5-24}$; 1,583.1 ± 95.2 nM for RyR2 plus PKA; and 125.1 ± 5.5 nM for RyR2 plus PKA and JTV519 (each n = 3; P < 0.05).

Discussion

The present study shows that the 1,4-benzothiazepine derivative JTV519 normalizes macromolecular complex composition and function of RyR channels in cardiac and skeletal muscle of mice with ischemia-induced HF. In calstabin-$2^{-/-}$ mice, JTV519 restored skeletal muscle function (for which calstabin-1 is required) but not cardiac muscle function, indicating that the therapeutic effect of the drug requires binding of calstabins to RyR. Our data suggest that JTV519 may improve cardiac and skeletal muscle function by reversing a maladaptive defect in intracellular Ca^{2+} signaling in HF. These studies are particularly significant considering that major symptoms in HF are caused by skeletal muscle dysfunction (shortness of breath due to diaphragmatic weakness and exercise intolerance due to skeletal muscle fatigue). Previous therapeutic approaches have targeted the cardiovascular system but not the skeletal muscle system. The present study raises the potential of a therapeutic target, RyR channels, that may be involved in defective function of cardiac and skeletal muscles. In addition, RyR is a therapeutic target that is involved in arrhythmogenesis (19). Therefore, the approach of preventing SR Ca^{2+} leak from the SR in cardiac and skeletal muscles may address the functional defects of both forms of striated muscle as well as inhibit arrhythmias.

RyR channels play an important physiological role in striated muscles, where they are required for SR Ca^{2+} release, which activates muscle contraction. The fight or flight response is an evolutionarily conserved stress pathway that involves activation of the sympathetic nervous system, leading to β-adrenergic stimulation of muscle. Binding of catecholamines to β-adrenergic receptors activates adenylyl cyclase by means of G proteins and increases the intracellular levels of the second messenger cAMP, which activates PKA. Previous studies have demonstrated that PKA phosphorylation activates mouse RyR2 channels by phosphorylation of Ser-2808

(7) and RyR1 channels by phosphorylation of Ser-2844 (10, 28). PKA phosphorylation of RyR2 causes dissociation of calstabin-2 from the channel (7). Accordingly, PKA phosphorylation of RyR1 dissociates calstabin-1 from the RyR channel complex (10).

A common feature of human HF and of many animal models of HF is a hyperadrenergic state, and elevated levels of circulating catecholamines correlate with increased mortality in HF patients (29). Chronic over-activity of the sympathetic nervous system in HF leads to PKA hyperphosphorylation of RyR2 (7, 9) and RyR1 in skeletal muscle (10). PKA hyperphosphorylation of RyR2 or RyR1 is associated with the depletion of the channel-stabilizing protein calstabin-2 or calstabin-1 in the channel complex, respectively (7, 10). RyR channels that are depleted of calstabin exhibit increased sensitivity to Ca^{2+}-induced activation and diastolic SR Ca^{2+} leak (7, 22). Diastolic SR Ca^{2+} leak along with reduced SR Ca^{2+} uptake due to down-regulation of SERCA2a could contribute to SR Ca^{2+} depletion that may explain the decreased contractility observed in failing hearts associated with reduced amplitude and slowed decay of the intracellular Ca^{2+} transient (30).

Previous studies have shown PKA hyperphosphorylation and reduced calstabin-2 binding to RyR2 in HF (7, 9, 21, 31). Other studies showed that calstabin-$2^{-/-}$ mice and patients with mutations in RyR2, which decrease calstabin-2 affinity for RyR2, develop exercise-induced arrhythmias (22). These data may raise the important question why calstabin-$2^{-/-}$ mice do not develop HF. It is well known that HF is a complex disease that involves changes in multiple signals in the body, including chronic activation of the sympathetic nervous system, which stresses many organs. Among the most prominent changes in HF, in addition to leaky RyR2, is down-regulation of the SR Ca^{2+} pump (SERCA2a), which conspires with leaky RyR2 to deplete the SR [Ca^{2+}] (32). The fact that catecholaminergic polymorphic ventricular tachycardia patients (who have mutations in RyR2 that reduce the binding affinity of calstabin-2 to the channel) and calstabin-$2^{-/-}$ mice do not exhibit HF suggests that RyR2 leak, by itself, may cause lethal cardiac arrhythmias, but not HF. The phenotype of calstabin-$2^{-/-}$ mice and catecholaminergic polymorphic ventricular tachycardia patients, combined with the results of the present study, suggest the following: (i) Leaky RyR2 by themselves can cause fatal cardiac arrhythmias not HF and (ii), combined with other cellular defects, including decreased SERCA2a activity, leaky RyR2 can promote the development of HF. The basis for the latter conclusion is that fixing the leak in RyR2 with JTV519 can improve HF. Thus, our model proposes that the diastolic RyR2 Ca^{2+} leak, in addition to causing lethal cardiac arrhythmias, contributes, along with many other changes, to cardiac dysfunction and HF progression. Diastolic Ca^{2+} leak through RyR2, which represents a maladaptive response due to chronic sympathetic nervous system activation, is a therapeutic target for a new class of drugs known as calcium channel stabilizers.

The fact that JTV519 did not improve cardiac function in calstabin-$2^{-/-}$ mice suggests that the therapeutic effect of JTV519 in HF depends on calstabin-2 binding to RyR2. In addition to enhancing calstabin binding to RyR, the 1,4-benzothiazepine derivative, JTV519, has been shown to inhibit annexin-V-dependent Ca^{2+} influx and to block voltage-gated Na^+, K^+, and Ca^{2+} channels (33, 34). Because none of these other known targets of JTV519 have been associated with therapeutic benefit in the treatment of HF, it is unlikely that these off-target activities of JTV519 are responsible for the beneficial effects of the drug in HF. However, we cannot exclude the possibility that JTV519 has another calstabin-2-dependent target that accounts for the beneficial effects observed in HF and exercise-induced cardiac arrhythmias (although there are no known calstabin-2-regulated proteins that could explain such an effect). The effectiveness of JTV519 is not limited to ischemia-induced HF, because this drug also induced reverse remodeling and decreased SR Ca^{2+} leak in a pacing-induced canine model of HF (24, 35). JTV519 may exert additional therapeutic effects in failing hearts. We have recently demonstrated that depletion of calstabin-2

from the RyR2 macromolecular complex, which is associated with increased RyR2 P_o, ventricular tachycardias, and sudden cardiac death in calstabin-$2^{+/-}$ haploinsufficient mice, could be reversed by treatment with JTV519 (19, 22). This finding is of particular interest considering that $\approx 50\%$ of patients with HF die suddenly because of cardiac arrhythmias (23). Moreover, patients with inherited mutations in RyR2 that decrease the affinity of the channel for calstabin-2 also develop triggered arrhythmias and sudden cardiac death (22, 36). Therefore, JTV519 may provide a specific way to treat contractile dysfunction and cardiac arrhythmias in patients with HF (19, 36).

Exercise intolerance and skeletal muscle weakness are major limiting symptoms in humans with chronic HF, and the existence of an intrinsic skeletal muscle defect has been suggested in patients with HF (37). Indeed, observed changes in skeletal muscle cells in HF include a decrease in oxidative enzymes, a shift from slow-twitch to fast-twitch fibers (38), and impaired O_2 utilization (39). In several cases, alterations in SR Ca^{2+} handling have been documented in skeletal muscle from experimental HF models (40, 41). Skeletal muscle Ca^{2+} transients in animals with HF typically exhibit reduced amplitude and a prolonged relaxation, consistent with altered expression levels of SERCA (41). However, these subtle changes of muscle protein levels often do not correlate well with the more extensive functional changes observed in muscles from HF subjects.

We have proposed that defects in SR Ca^{2+} release channel function may provide a mechanism that could contribute to the impaired skeletal muscle function in HF (10). Studies from our laboratory have demonstrated defective function of RyR1 channels in HF skeletal muscle, which were analogous to those found in RyR2 channels in failing myocardium: PKA hyperphosphorylation

of RyR1 and depletion of calstabin-1 (10, 27). These findings suggest that defects in RyR1 function could alter intracellular Ca^{2+} handling and contribute to early fatigue in HF skeletal muscle (40). The present study shows that fixing the defect in RyR1 results in improved performance of HF skeletal muscle, providing important support for the model in which defective regulation of RyR1 plays a role in HF symptoms, including shortness of breath and reduced exercise tolerance. The finding that skeletal muscle fatigability was improved in the calstabin-$2^{-/-}$ mice, in which cardiac function was not enhanced by JTV519, highlights the unique and independent pharmacological effects of JTV519 on skeletal and cardiac muscle function in HF (calstabin-1, which stabilizes the closed state of the skeletal RyR1, is not affected in calstabin-$2^{-/-}$ mice). Future studies will be required to assess whether increased calstabin-1 binding to RyR1 in mice with HF also improves exercise tolerance.

In conclusion, the present study provides a mechanism for treating ischemia-induced HF that targets RyR channels in cardiac and skeletal muscles. The approach is based on enhancing the binding of the stabilizing protein calstabin to the PKA-hyperphosphorylated RyR channel and provides strong evidence in support of the RyR leak hypothesis as a contributor to the pathogenesis of HF. Moreover, the present study establishes that the mechanism of action of JTV519 in HF involves calstabin binding to RyR. Increased calstabin-1 binding to RyR1 may represent a method to treat skeletal muscle dysfunction in HF.

1. Hunt, S. A., Baker, D. W., Chin, M. H., Cinquegrani, M. P., Feldman, A. M., Francis, G. S., Ganiats, T. G., Goldstein, S., Gregoratos, G., Jessup, M. L., *et al.* (2001) *J. Am. Coll. Cardiol.* **38,** 2101–2113.
2. McKenzie, D. B. & Cowley, A. J. (2003) *Postgrad. Med. J.* **79,** 634–642.
3. Kramer, R. S., Mason, D. T. & Braunwald, E. (1968) *Circulation* **38,** 629–634.
4. Harrington, D. & Coats, A. J. (1997) *Curr. Opin. Cardiol.* **12,** 224–232.
5. Bers, D. M., Eisner, D. A. & Valdivia, H. H. (2003) *Circ. Res.* **93,** 487–490.
6. Piacentino, V., III, Weber, C. R., Chen, X., Weisser-Thomas, J., Margulies, K. B., Bers, D. M. & Houser, S. R. (2003) *Circ. Res.* **92,** 651–658.
7. Marx, S. O., Reiken, S., Hisamatsu, Y., Jayaraman, T., Burkhoff, D., Rosemblit, N. & Marks, A. R. (2000) *Cell* **101,** 365–376.
8. Pogwizd, S. M. & Bers, D. M. (2002) *Ann. N. Y. Acad. Sci.* **976,** 454–465.
9. Yano, M., Ono, K., Ohkusa, T., Suetsugu, M., Kohno, M., Hisaoka, T., Kobayashi, S., Hisamatsu, Y., Yamamoto, T., Noguchi, N., *et al.* (2000) *Circulation* **102,** 2131–2136.
10. Reiken, S., Lacampagne, A., Zhou, H., Kherani, A., Lehnart, S. E., Ward, C., Huang, F., Gaburjakova, M., Gaburjakova, J., Rosemblit, N., *et al.* (2003) *J. Cell Biol.* **160,** 919–928.
11. Shannon, T. R., Pogwizd, S. M. & Bers, D. M. (2003) *Circ. Res.* **93,** 592–594.
12. Jiang, M. T., Lokuta, A. J., Farrell, E. F., Wolff, M. R., Haworth, R. A. & Valdivia, H. H. (2002) *Circ. Res.* **91,** 1015–1022.
13. Eisner, D. A. & Trafford, A. W. (2002) *Circ. Res.* **91,** 979–981.
14. Xiao, B., Sutherland, C., Walsh, M. P. & Chen, S. R. (2004) *Circ. Res.* **94,** 487–495.
15. Fill, M. & Copello, J. A. (2002) *Physiol. Rev.* **82,** 893–922.
16. Kaftan, E., Marks, A. R. & Ehrlich, B. E. (1996) *Circ. Res.* **78,** 990–997.
17. Jayaraman, T., Brillantes, A. M., Timerman, A. P., Erdjument-Bromage, H., Fleischer, S., Tempst, P. & Marks, A. R. (1992) *J. Biol. Chem.* **267,** 9474–9477.
18. Wehrens, X. H. & Marks, A. R. (2003) *Trends Biochem. Sci.* **28,** 671–678.
19. Wehrens, X. H., Lehnart, S. E., Reiken, S. R., Deng, S. X., Vest, J. A., Cervantes, D., Coromilas, J., Landry, D. W. & Marks, A. R. (2004) *Science* **304,** 292–296.
20. Brillantes, A. B., Ondrias, K., Scott, A., Kobrinsky, E., Ondriasova, E., Moschella, M. C., Jayaraman, T., Landers, M., Ehrlich, B. E. & Marks, A. R. (1994) *Cell* **77,** 513–523.
21. Reiken, S., Wehrens, X. H., Vest, J. A., Barbone, A., Klotz, S., Mancini, D., Burkhoff, D. & Marks, A. R. (2003) *Circulation* **107,** 2459–2466.
22. Wehrens, X. H., Lehnart, S. E., Huang, F., Vest, J. A., Reiken, S. R., Mohler, P. J., Sun, J., Guatimosim, S., Song, L. S., Rosemblit, N., *et al.* (2003) *Cell* **113,** 829–840.
23. Zipes, D. P. & Wellens, H. J. J. (1998) *Circ* **98,** 2334–2351.
24. Yano, M., Kobayashi, S., Kohno, M., Doi, M., Tokuhisa, T., Okuda, S., Suetsugu, M., Hisaoka, T., Obayashi, M., Ohkusa, T. & Matsuzaki, M. (2003) *Circulation* **107,** 477–484.
25. van Rooij, E., Doevendans, P. A., Crijns, H. J., Heeneman, S., Lips, D. J., van Bilsen, M., Williams, R. S., Olson, E. N., Bassel-Duby, R., Rothermel, B. A. & De Windt, L. J. (2004) *Circ. Res.* **94,** e18–e26.
26. Reiken, S., Gaburjakova, M., Guatimosim, S., Gomez, A. M., D'Armiento, J., Burkhoff, D., Wang, J., Vassort, G., Lederer, W. J. & Marks, A. R. (2003) *J. Biol. Chem.* **278,** 444–453.
27. Ward, C. W., Reiken, S., Marks, A. R., Marty, I., Vassort, G. & Lacampagne, A. (2003) *FASEB J.* **17,** 1517–1519.
28. Suko, J., Maurer-Fogy, I., Plank, B., Bertel, O., Wyskovsky, W., Hohenegger, M. & Hellmann, G. (1993) *Biochim. Biophys. Acta* **1175,** 193–206.
29. Cohn, J. N., Levine, T. B., Olivari, M. T., Garberg, V., Lura, D., Francis, G. S., Simon, A. & Rector, T. (1984) *N. Engl. J. Med.* **311,** 819–823.
30. Beuckelmann, D. J., Nabauer, M. & Erdmann, E. (1992) *Circulation* **85,** 1046–1055.
31. Ono, K., Yano, M., Ohkusa, T., Kohno, M., Hisaoka, T., Tanigawa, T., Kobayashi, S. & Matsuzaki, M. (2000) *Cardiovasc. Res.* **48,** 323–331.
32. Hasenfuss, G., Reinecke, H., Studer, R., Meyer, M., Pieske, B., Holtz, J., Holubarsch, C., Posival, H., Just, H. & Drexler, H. (1994) *Circ. Res.* **75,** 434–442.
33. Kiriyama, K., Kiyosue, T., Wang, J. C., Dohi, K. & Arita, M. (2000) *Naunyn-Schmiedeberg's Arch. Pharmacol.* **361,** 646–653.
34. Inagaki, K., Kihara, Y., Izumi, T. & Sasayama, S. (2000) *Cardiovasc. Drugs Ther.* **14,** 489–495.
35. Kohno, M., Yano, M., Kobayashi, S., Doi, M., Oda, T., Tokuhisa, T., Okuda, S., Ohkusa, T. & Matsuzaki, M. (2003) *Am. J. Physiol.* **284,** H1035–H1042.
36. Lehnart, S. E., Wehrens, X. H. T., Laitinen, P. J., Reiken, S. R., Deng, S. X., Chen, Z., Landry, D. W., Kontula, K., Swan, H. & Marks, A. R. (2004) *Circulation*, r113–r119.
37. Minotti, J. R., Christoph, I., Oka, R., Weiner, M. W., Wells, L. & Massie, B. M. (1991) *J. Clin. Invest.* **88,** 2077–2082.
38. Mancini, D. M., Coyle, E., Coggan, A., Beltz, J., Ferraro, N., Montain, S. & Wilson, J. R. (1989) *Circulation* **80,** 1338–1346.
39. Bernocchi, P., Cargnoni, A., Vescovo, G., Dalla Libera, L., Parrinello, G., Boraso, A., Ceconi, C. & Ferrari, R. (2003) *Basic Res. Cardiol.* **98,** 114–123.
40. Lunde, P. K., Dahlstedt, A. J., Bruton, J. D., Lannergren, J., Thoren, P., Sejersted, O. M. & Westerblad, H. (2001) *Circ. Res.* **88,** 1299–1305.
41. Peters, D. G., Mitchell, H. L., McCune, S. A., Park, S., Williams, J. H. & Kandarian, S. C. (1997) *Circ. Res.* **81,** 703–710.

Table 1. Mean and SEM for each genotype, operative, and treatment group

	Wild-type				Calstabin-2^{-/-}			
	Sham		Myocardial infarction		Sham		Myocardial infarction	
	Placebo	JTV519	Placebo	JTV519	Placebo	JTV519	Placebo	JTV519
Biometric values								
Mice studied, n	10	8	16	13	9	10	11	16
Survival, %	100%	100%	81%	85%	100%	100%	64%	44%
Body weight, g	26.4±1.7	25.1±0.4	27.4±0.9	28.2±0.5	26.1±1.7	25.0±0.6	23.7±1.0	26.3±1.4
HW/BW, mg/g	5.2±0.3	5.3±0.2	9.0±0.6	7.7±0.4*	5.4±0.3	5.3±0.2	9.2±0.8	9.0±0.6
HW/TL, mg/mm	7.2±0.8	6.9±0.2	13.5±1.0	11.6±0.7*	6.9±0.1	6.9±0.3	12.3±0.9	12.2±1.0
Infarct size	0	0	39.0±1.9	40.7±3.7	0	0	41.8±4.7	46.4±5.1
Echocardiography								
LVPW, μm	76±2.7	74±2.8	76.9±2.3	76±2.3	73±2.3	71±2.3	76±3.1	73±2.9
EDD, mm	0.37±0.02	0.36±0.01	0.56±0.02	0.54±0.03	0.35±0.01	0.36±0.02	0.51±0.03	0.50±0.02
ESD, mm	0.28±0.02	0.26±0.01	0.46±0.04	0.47±0.03	0.24±0.01	0.24±0.01	0.44±0.03	0.45±0.02
EF, %	63.3±3.1	66.7±4.9	31.1±3.1	45.8±5.1*	69.1±3.1	68.6±2.8	31.5±5.7	31.9±3.1
FS, %	29.8±2.2	32.2±3.7	12.5±1.3	20.2±2.9*	30.5±5.0	33.3±2.0	12.9±2.8	12.8±1.5
EDV, μl	0.12±0.01	0.10±0.01	0.41±0.04	0.36±0.05	0.09±0.01	0.11±0.01	0.32±0.08	0.32±0.03
Hemodynamic data								
MAP, mmHg	75.9±6.4	70.2±3.4	67.1±2.7	68.5±3.4	76.3±5.1	72.8±4.7	67.9±4.7	68.2±4.7
HR, min^{-1}	480±13	477±12	493±24	458±33	460±9	465±14	471±28	457±21
ESP, mmHg	94.8±2.7	93.9±1.5	84.0±3.1	92.7±5.4*	101±3.4	94.8±2.2	83.2±4.0	79.0±3.2
dP/dt(max)	8005±284	8878±350	6215±309	6826±735	8515±473	8030±322	5907±446	5726±314
dP/dt(min)	-6530±419	-7371±266	-5249±353	-5810±649	-7506±382	-7068±407	-4878±301	-4481±327

Data are presented as mean ± SEM. HW, heart weight; BW, body weight; TL, tibia length; LVPW, left ventricular posterior wall thickness; EDD, end-diastolic diameter; ESD, end-systolic diameter; EF, ejection fraction; FS, fractional shortening; EDV, end-diastolic volume; MAP, mean arterial blood pressure; HR, heart rate; ESP, end-systolic pressure.

*$P < 0.05$ placebo versus JTV519.

A

JTV519 (nM)	0	10	20	50	100	200	500	1000
PKI	+	-	-	-	-	-	-	-
Calstabin	-	+	+	+	+	+	+	+

Calstabin1 — 15 kDa

Calstabin2 — 15 kDa

B

RyR2 - calstabin2

RyR1 - calstabin1

□ PKA + PKI
○ PKA
● PKA + JTV519

Bound/Free (pmol/mg - µM)

Bound (pmol/mg protein)